

the proposed concerted unimolecular fragmentation step explains the effects of structure, conformation, counterion, and solvent on regioselectivity without any need to resort to the hypothesis of an unsubstantiated σ^* intermediate.

Experimental Section

Samples of compounds 1-3 and 5 were kindly provided by Prof. A. Maercker, 4 was purchased from Aldrich, and 6 and 7 were synthesized and purified as described in the literature.^{39,40}

Tetrahydrofuran (THF) and 1,2-dimethoxyethane (DME) were distilled from a Na-K alloy in the vacuum line directly into the sample tube.

- (36) Amatore, C.; Combellas, C.; Pinson, J.; Oturan, M. A.; Robveille, S.; Savéant, J.-M.; Thiébaud, A. *J. Am. Chem. Soc.* **1985**, *107*, 4846.
 (37) Symons, M. C. R. *J. Chem. Soc., Chem. Commun.* **1977**, 408.
 (38) Symons, M. C. R. *Pure Appl. Chem.* **1981**, *53*, 223.
 (39) Willner, I.; Halpern, M. *Synthesis* **1979**, 177.
 (40) Meek, J. S.; Monroe, P. A.; Bouboulis, C. J. *J. Org. Chem.* **1963**, *28*, 2572.

The radicals have been generated by alkali-metal reduction (Na-K alloy, Li, Na, K, and Cs) under high vacuum with standard techniques.²⁸

ESR, ENDOR, and TRIPLE resonance studies were recorded on a Bruker ER 200-D instrument for ESR and a Bruker EN 810 spectrometer system for ENDOR and TRIPLE resonance.

Acknowledgment. We thank the Instituto Nacional de Investigação Científica (INIC), Portugal, for financial support through Centro de Processos Químicos da Universidade Técnica de Lisboa and the Foundation Volkswagenwerke, Germany, for a cooperative research grant with the University of Siegen, Professor Adalbert Maercker, University of Siegen, provided us with information on the extensive systematic preparative work of his collaborators, prior to the publication of his review article,⁵ where these experiments were reported for the first time in public. We thank him for this, for sending us samples of several ethers, and for encouraging us to reopen the discussion on the mechanism of ether cleavage by alkali metals. B.J.H. also thanks Professor Andrew Streitwieser, UCLA, for a stimulating discussion.

Deprotonation of Tertiary Amine Cation Radicals. A Direct Experimental Approach

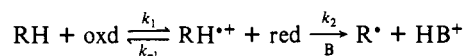
J. P. Dinnocenzo*[†] and T. E. Banach[‡]

*Contribution from the Department of Chemistry, University of Rochester, Rochester, New York 14627. Received March 30, 1989.
 Revised Manuscript Received June 26, 1989*

Abstract: The tertiary amine cation radical salt $p\text{-An}_2\text{NCH}_3^{+\bullet}\text{AsF}_6^-$ was prepared by oxidation of the corresponding amine with dioxygenyl hexafluoroarsenate. The cation radical salt was characterized by EPR spectroscopy, by magnetic susceptibility, by UV-vis spectroscopy, and by single-crystal X-ray diffraction. The reaction of the salt with quinuclidine produced at 1:1 ratio of $p\text{-An}_2\text{NCH}_3^{+\bullet}$ and the adduct 1. Four possible mechanisms were considered for this reaction: a proton-transfer mechanism, an electron-transfer mechanism, and two mechanisms involving a cation radical/base complex. Stopped-flow kinetics were used to determine that the reaction rate was first-order in $p\text{-An}_2\text{NCH}_3^{+\bullet}\text{AsF}_6^-$ and first-order in quinuclidine. A comparison of the reaction rate for $p\text{-An}_2\text{NCH}_3^{+\bullet}\text{AsF}_6^-$ vs $p\text{-An}_2\text{NCD}_3^{+\bullet}\text{AsF}_6^-$ provided an isotope effect of 7.68 (7) at 15.1 °C. The combined kinetic data ruled out all but a rate-limiting proton-transfer mechanism. The temperature dependence of the reaction rate provided activation parameters for the deprotonation: $\Delta H^\ddagger = 3.7$ (1) kcal/mol and $\Delta S^\ddagger = -22.3$ (4) cal/mol-deg. Reaction of $p\text{-An}_2\text{NCH}_3^{+\bullet}\text{AsF}_6^-$ with four substituted quinuclidine bases provided a Brønsted β of 0.63. The isotope effects for reaction with the substituted quinuclidine bases were measured, and a plot of $k_{\text{H}}/k_{\text{D}}$ vs $\text{p}K_{\text{a}}$ was found to have a maximum ca. 8 $\text{p}K_{\text{a}}$ units lower than the $\text{p}K_{\text{a}}$ of the cation radical. This was explained in terms of the differing widths of the potential energy wells for the X-H bonds being broken and being made.

Deprotonation at carbon is a commonly proposed reaction for many organic cation radical intermediates. For example, this is the generally accepted fate of alkylaromatic and tertiary amine cation radicals generated in chemical,¹ electrochemical,² photochemical,³ and even some enzymatic oxidation reactions.⁴ Despite their importance, these proton-transfer reactions are still poorly understood vis-à-vis comparable proton transfers from even electron molecules.

Part of the difficulty in probing cation radical deprotonations is that they are often masked by prior electron-transfer steps. In order to extract kinetic data regarding the deprotonation step, it is usually necessary to make some sort of approximation. For example, consider the frequently encountered kinetic scheme shown below. For situations where the deprotonation step is rate-limiting, one needs to know either the electron-transfer equilibrium constant (k_1/k_{-1}) or the rate constant for the back-electron-transfer step (k_{-1}) in order to relate the observed reaction rate constant to the deprotonation rate constant (k_2). In practice, this is often difficult to do. One of the problems is that thermodynamically meaningful oxidation potentials are difficult to obtain for the substrates of interest.⁵



We have been exploring a way to more directly examine the deprotonation of organic cation radicals that circumvents the

(1) Alkylaromatics: (a) Schlesener, C. J.; Amatore, C.; Kochi, J. K. *J. Am. Chem. Soc.* **1984**, *106*, 7472 and references therein. Tertiary amines: (b) Chow, Y. L.; Danen, W. C.; Nelsen, S. F.; Rosenblatt, D. H. *Chem. Rev.* **1978**, *78*, 243 and references therein.

(2) Alkylaromatics: (a) Nyberg, K. In *Encyclopedia of Electrochemistry of the Elements*; Bard, A. J., Lund, H., Eds.; Marcel Dekker: New York, 1978; Vol. XI, Chapter IX-1, p 43. (b) Ebersson, L.; Nyberg, K. *Acc. Chem. Res.* **1973**, *6*, 106. (c) Baumberger, R. S.; Parker, V. D. *Acta Chem. Scand., Ser. B* **1980**, *B34*, 537. (d) Bewick, A.; Edwards, G. J.; Mellor, J. M.; Pons, S. J. *Chem. Soc., Perkin Trans. 2* **1977**, 1952. Tertiary amines: (e) Weinberg, N. L.; Weinberg, H. R. *Chem. Rev.* **1968**, *68*, 449. (f) Mann, C. K.; Barnes, K. K. *Electrochemical Reactions in Nonaqueous Systems*; Marcel Dekker: New York, 1970; Chapter 9. (g) Masui, M.; Sayo, H. *J. Chem. Soc. B* **1971**, 1593.

(3) Alkylaromatics: (a) Mariano, P. S.; Stavinola, J. L. In *Synthetic Organic Photochemistry*; Horspool, W. M., Ed.; Plenum Press: New York, 1984; Chapter 3 and references therein. (b) Lewis, F. D. *Acc. Chem. Res.* **1986**, *19*, 401 and references therein. Tertiary amines: (c) Cohen, S. G.; Parola, A.; Parsons, G. H., Jr. *Chem. Rev.* **1973**, *73*, 141. (d) Wagner, P. J. *Top. Curr. Chem.* **1976**, *66*, 1. (e) Davidson, R. S. *Adv. Phys. Org. Chem.* **1983**, *19*, 1. (f) Reference 3a. (g) Reference 3b. (h) Kavarnos, G. J.; Turro, N. J. *Chem. Rev.* **1986**, *86*, 401.

[†] Fellow of the Alfred P. Sloan Foundation, 1988-90.

[‡] Weissberger Fellow, 1987-88.

complications associated with prior electron-transfer steps. Our approach is to prepare isolable cation radical salts and then to examine their reactions with various bases. The preparation of these salts requires, of course, an oxidation procedure that generates cation radicals under nonbasic and nonnucleophilic conditions. We recently developed such a procedure that uses dioxygenyl cation salts (e.g., $O_2^{++}AsF_6^-$) as one-electron oxidants.⁶

We describe here our work on the reaction of a series of substituted quinuclidine bases with an isolable tertiary amine cation radical salt, $p-An_2NCH_3^{++}AsF_6^-$. This salt has enabled us to obtain directly, for the first time, rate constants for the deprotonation of a tertiary amine cation radical, as well as other mechanistic information, e.g., activation parameters, isotope effects, and Brønsted parameters.

Tertiary amine cation radical deprotonations have been the subject of considerable discussion in the recent literature. Most recently, Nelsen and Ippoliti have argued that the high kinetic acidity previously proposed for tertiary amine cation radicals might be incorrect.⁷ On the basis of a thermodynamic acidity estimate, these authors concluded that these cation radicals are not extremely acidic and that they may often decompose by pathways other than deprotonation. Of course, one concern regarding this conclusion is that the relationship between the thermodynamic and kinetic acidity of these cation radicals is not clear. A more serious concern is that the pK_a calculated for the tertiary amine cation radical in this study may have been overestimated by as much as 10 pK_a units.⁸ If the correction is indeed this large, it might well alter the authors' conclusions.

A low kinetic acidity for tertiary amine cation radicals appears inconsistent with the results of Sinha and Bruice who have estimated the rate constants for deprotonation of the *N*-methylacridan cation radical by several bases.¹⁰ The cation radical was generated by ferricyanide oxidation of the amine, and the reaction was found to obey a kinetic scheme similar to that shown above. Making the assumption that the rate constant for back-electron transfer (k_{-1}) from ferrocyanide to the *N*-methylacridan cation radical was diffusion-controlled, the authors were able to estimate the rate constants for deprotonation. They found large deprotonation rates ($k_2 \approx 10^6-10^7 M^{-1} s^{-1}$) even for rather weak bases (e.g., acetate, formate, and imidazole). These data suggest that proton transfer from tertiary amine cation radicals may be rapid. One should bear in mind, however, that these rate constant estimates rest on an assumption regarding the back-electron-transfer rate.

In order to more directly quantify the deprotonation rates of tertiary amine cation radicals, we decided to prepare a stable cation radical salt and examine its reaction with bases. Described below are our first experiments along these lines.

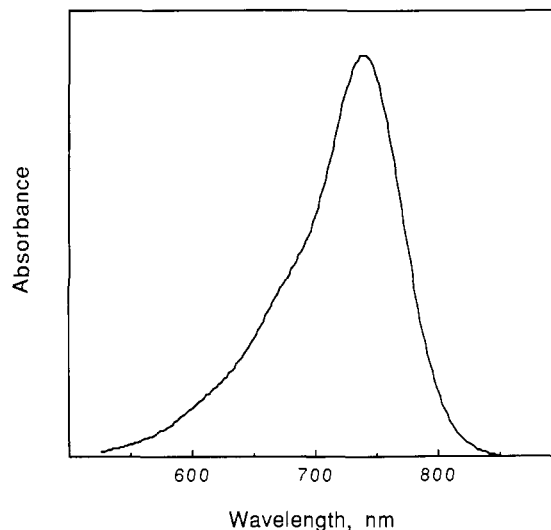


Figure 1. UV-vis spectrum of $p-An_2NCH_3^{++}AsF_6^-$ in acetonitrile.

Table I. Crystallographic Data for $p-An_2NCH_3^{++}AsF_6^-$

empirical formula	$C_{15}H_{17}NO_2AsF_6$
cryst syst	monoclinic
space gp	$C2/c$
a , Å	14.700 (8)
b , Å	15.374 (4)
c , Å	8.78 (1)
β , deg	117.47 (6)
V , Å ³	1760 (5)
Z	4
ρ (calcd), g cm ⁻³	1.63
temp, °C	23
$F(000)$	868
diffractometer	Enraf-Nonius CAD-4
radiatn, Å	Mo $K\alpha$, $\lambda = 0.71069$ with graphite
scan mode	ω
2θ range, deg	$4 \leq 2\theta \leq 50$
data coll'd	$\pm h, +k, +l$
scan speed, deg/min	2.5
reflns coll'd	1686
independent data	1620
independent data obs'd, $I > 3\sigma(I)$	1154
R , %	3.8
R_w , %	4.8
GOF	1.48
$\Delta(\rho)$, e Å ⁻³	0.44
no. of variable param	155
max peak in final diff Fourier, e Å ⁻³	0.72

Results and Discussion

Preparation and Characterization of Cation Radical Salt. As described above, we prepared the cation radical salt used in this study, $p-An_2NCH_3^{++}AsF_6^-$, by oxidation of the neutral amine with $O_2^{++}AsF_6^-$ in chlorodifluoromethane. The hyperfine splitting constants obtained from its EPR spectrum were closely similar to those previously reported under electrolytic flow conditions.¹¹ Solutions containing the cation radical salt were intensely green, and the salt crystallized from methylene chloride/diethyl ether to give purple needles.

Solutions of the salt were further characterized by magnetic susceptibility measurements in methylene chloride using the Evans NMR shift method.¹² The observed and calculated paramagnetic solvent shifts were within 3% of that expected and demonstrate that the cation radical does not form a diamagnetic dimer to any appreciable extent.¹³

(4) Alkylaromatics: (a) Guengerich, F. P.; Macdonald, T. L. *Acc. Chem. Res.* **1984**, *17*, 9 and references therein. Tertiary amines: (b) Silverman, R. B.; Hoffman, S. J.; Catus, W. B., III *J. Am. Chem. Soc.* **1980**, *102*, 7126. (c) Shannon, P.; Bruice, T. C. *J. Am. Chem. Soc.* **1981**, *103*, 4580. (d) Shono, T.; Toda, T.; Oshino, N. *J. Am. Chem. Soc.* **1982**, *104*, 2639. (e) Miwa, G. T.; Walsh, J. S.; Kedderis, G. L.; Hollenberg, P. F. *J. Biol. Chem.* **1983**, *258*, 14445. (f) Reference 4a. (g) Burka, L. T.; Guengerich, F. P.; Willard, R. J.; Macdonald, T. L. *J. Am. Chem. Soc.* **1985**, *107*, 2549. (h) Wimalasena, K.; May, S. W. *J. Am. Chem. Soc.* **1987**, *109*, 4036.

(5) For a rare exception, see: Schlesener, C. J.; Amatore, C.; Kochi, J. K. *J. Phys. Chem.* **1986**, *90*, 3747.

(6) (a) Dinnocenzo, J. P.; Banach, T. E. *J. Am. Chem. Soc.* **1986**, *108*, 6063. (b) Dinnocenzo, J. P.; Banach, T. E. *J. Am. Chem. Soc.* **1988**, *110*, 971.

(7) Nelsen, S. F.; Ippoliti, J. T. *J. Am. Chem. Soc.* **1986**, *108*, 4879.

(8) The pK_a estimated in ref 7 should be corrected by two factors. First, the amine oxidation potential should have been referenced to NHE rather than to SCE.⁹ Second, the bond dissociation free energy for the α -C-H bond should have been used instead of the bond dissociation enthalpy.⁹ Both of these corrections lower the calculated pK_a . The first correction is 0.24 V ($-4.1 pK_a$ units). The second correction requires an estimate of the bond dissociation entropy. This may be approximated by the standard entropy of the hydrogen atom (27.4 cal/mol-deg).⁹ At 25 °C this corresponds to 8.2 kcal/mol and results in a lowering of the calculated pK_a by 6 pK_a units. Thus the total correction is ca. 10 pK_a units.

(9) Nicholas, A. M. de P.; Arnold, D. R. *Can. J. Chem.* **1982**, *60*, 2165.

(10) Sinha, A.; Bruice, T. C. *J. Am. Chem. Soc.* **1984**, *106*, 7291.

(11) Seo, E. T.; Nelson, R. F.; Fritsch, J. M.; Marcoux, L. S.; Leedy, D. W.; Adams, R. N. *J. Am. Chem. Soc.* **1966**, *88*, 3498.

(12) (a) Evans, D. F. *J. Chem. Soc.* **1959**, 2003. (b) Live, D. H.; Chan, S. I. *Anal. Chem.* **1970**, *42*, 791. (c) Becconsall, J. K.; Daves, G. D., Jr.; Anderson, W. R., Jr. *J. Am. Chem. Soc.* **1970**, *92*, 430.

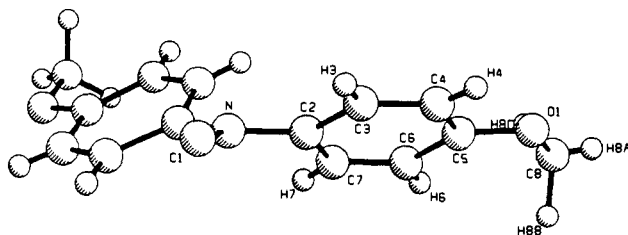


Figure 2. Molecular structure of the aminium ion fragment of $p\text{-An}_2\text{NCH}_3^+\text{AsF}_6^-$.

Table II. Selected Bond Distances and Bond Angles for $p\text{-An}_2\text{NCH}_3^+\text{AsF}_6^-$ ^a

bond	distance, Å	bond	angle, deg
N-C1	1.452 (7)	C1-N-C2	119.7 (2)
N-C2	1.401 (4)	C2-N-C2'	120.6 (4)
C2-C3	1.408 (5)	C7-C2-N	120.5 (3)
C2-C7	1.389 (5)	C7-C2-C3	118.7 (4)
C3-C4	1.361 (6)	N-C2-C3	120.8 (3)
C4-C5	1.386 (5)	C4-C3-C2	119.9 (4)
C5-C6	1.394 (5)	C3-C4-C5	120.8 (4)
C6-C7	1.371 (6)	C4-C5-C6	120.0 (4)
O1-C5	1.353 (4)	O1-C5-C6	124.1 (3)
O1-C8	1.429 (6)	O1-C5-C4	115.9 (3)
		C7-C6-C5	119.1 (4)
		C6-C7-C2	121.3 (4)
		C5-O1-C8	117.3 (4)

^aSee Figure 2 for the numbering scheme.

The UV-vis spectrum of the salt in acetonitrile (Figure 1) had a maximum in the visible region at 734 nm ($\log \epsilon = 4.33$). It is worth pointing out that dilution of the cation radical salt to the concentrations necessary to achieve reasonable absorbance values resulted in some decomposition of the cation radical. This was inferred from negative deviations in Beer's law plots upon successive dilutions. Empirically we discovered a way to prevent this decomposition. We found that good Beer's law plots could be obtained by the addition of $n\text{-Bu}_4\text{N}^+\text{AsF}_6^-$ to the acetonitrile. The inclusion of the ammonium salt did *not* detectably affect λ_{max} of the cation radical. We do not know by what mechanism the ammonium salt "preserves" the amine cation radical salt. One possibility is that it sequesters basic or nucleophilic impurities in the acetonitrile by an ion-pairing process. Finally, we should point out that the absorption maximum of the cation radical is solvent-dependent. For example, λ_{max} in methylene chloride is shifted 30 nm to 764 nm ($\log \epsilon = 4.43$).

Final structural confirmation of the cation radical salt was secured by a single-crystal X-ray diffraction analysis. The important crystallographic parameters are provided in Table I. The structure of the cation radical is shown in Figure 2, and bond distances and bond angles are given in Table II. As expected for an unconstrained tertiary amine cation radical, the central nitrogen and its three directly bonded carbon atoms all lie in a common plane. The dihedral angle between this plane and that of the aromatic rings is 31° and defines the twist angle of the aromatic rings.

The crystal structure of the cation radical gave us the opportunity to try to estimate the structural effect of oxidation on the *N*-methyl protons. The large EPR hyperfine splitting constant attributed to these protons suggested that they interact strongly with the unpaired electron. Unfortunately, the local C_3 axis through the methyl group combined with the global C_2 symmetry of the amine cation radical resulted in a necessary disorder of the methyl protons. In practice, we could not adequately refine them so we did not pursue this goal further.

Reaction of Cation Radical Salt with Bases. Although $p\text{-An}_2\text{NCH}_3^+\text{AsF}_6^-$ was indefinitely stable in acetonitrile solution,

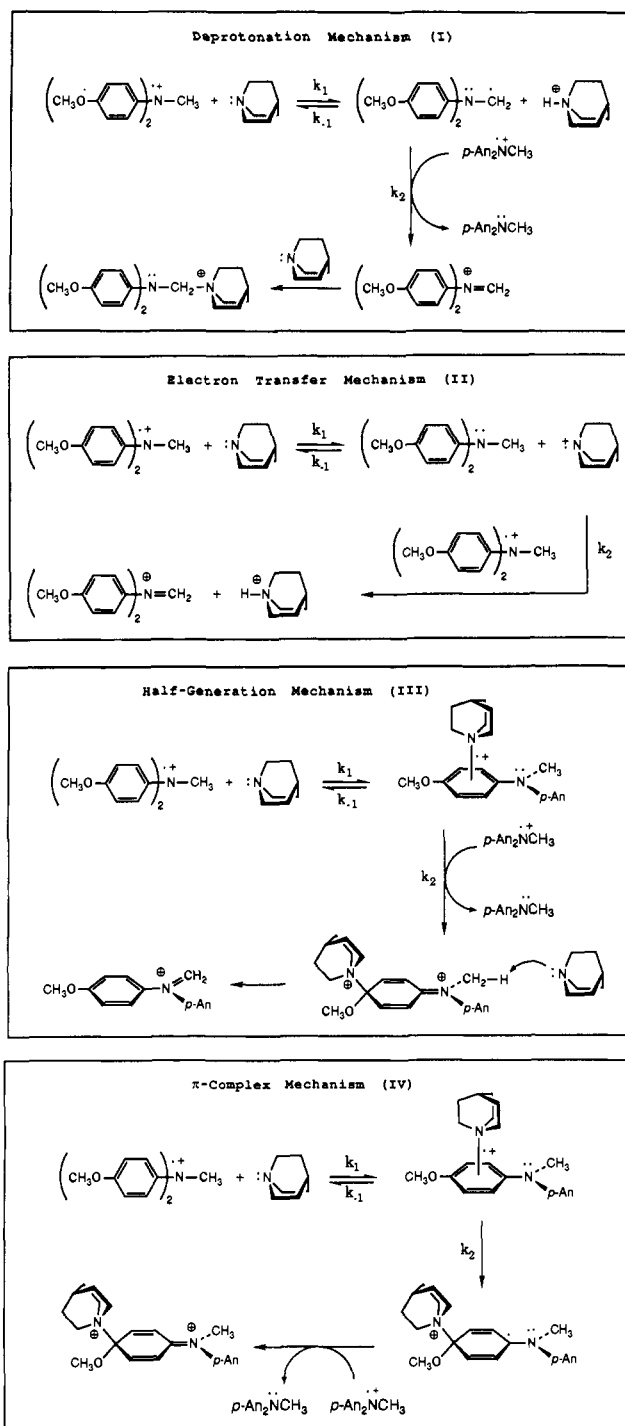
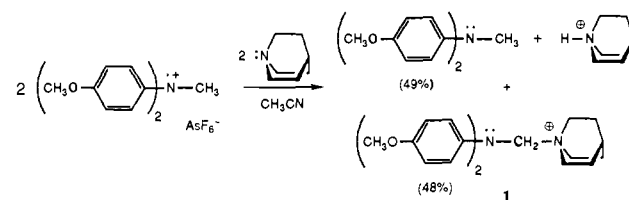


Figure 3. Four possible mechanisms for the reaction of $p\text{-An}_2\text{NCH}_3^+$ with quinuclidine.

it rapidly reacted when quinuclidine was added. The stoichiometry of the reaction is shown below.



The products derived from the amine cation radical were the corresponding neutral amine and adduct **1**. Both products were formed in an essentially 1:1 ratio and in high overall yield. The structural assignment of **1** was made by ^1H NMR spectroscopy and by independent synthesis (vide infra).

(13) See, for example: (a) Kawamori, A.; Honda, A.; Joo, N.; Suzuki, K.; Oshika, Y. *J. Chem. Phys.* **1966**, *44*, 4363. (b) Sorgo, M. de; Wasserman, B.; Szwarc, M. *J. Phys. Chem.* **1972**, *76*, 3468.

These reaction products might be explained by any of the four possible reaction mechanisms shown in Figure 3. We first consider the deprotonation mechanism. This mechanism involves initial proton transfer from the aminium ion to quinuclidine to produce an α -amino radical and the quinuclidinium ion. The α -amino radical is strongly reducing ($E_p = -0.79$ V vs SCE) and would be expected to be rapidly oxidized by the p -An₂NCH₃^{•+} present to form an iminium ion and the neutral amine. The iminium ion might then be transformed into **1** by addition of quinuclidine. This last possibility was tested independently. We prepared p -An₂N=CH₂⁺BF₄⁻ and showed that it rapidly reacted with quinuclidine to provide the same product attributed to **1**.

The second reaction mechanism ("electron transfer") involves an initial electron transfer from quinuclidine to p -An₂NCH₃^{•+}. This step is then followed by the quinuclidine cation radical abstracting a hydrogen atom from p -An₂NCH₃^{•+} to produce p -An₂N=CH₂[•]. Alternatively, the abstraction could occur from p -An₂NCH₃, which would produce an α -amino radical. This radical would have the same fate as in the deprotonation mechanism. As we will discuss further below, the homolytic bond dissociation energy of the *N*-methyl C-H bond in p -An₂NCH₃^{•+} is significantly weaker than that in p -An₂NCH₃. Thus the hydrogen atom abstraction by the quinuclidine cation radical might be expected to be faster from p -An₂NCH₃^{•+}, even though it involves a reaction of two positively charged species.

The third mechanism ("half-generation") is based, in part, on the mechanism previously elucidated for the reaction of several aromatic cation radicals with nucleophiles.¹⁴ It involves the formation of a cation radical/nucleophile complex—shown here as a π -complex—which is subsequently oxidized by aminium ion to form a dication and the neutral amine. The dication could then react with quinuclidine via an elimination mechanism to form the iminium ion, which subsequently would be trapped by quinuclidine. The location of the quinuclidine moiety in the dication is arbitrarily illustrated at the para position of the *p*-anisyl ring. Alternatively, it could be placed at either of the vinylogous ortho positions or at the aryl amine nitrogen.

The fourth mechanism (" π -complex") is a variant on the half-generation mechanism in which the amine cation radical/quinuclidine complex is proposed to undergo a unimolecular rearrangement instead of an oxidation. The rearranged complex may be viewed as an α -amino radical, which, as in the deprotonation mechanism, might be expected to be oxidized by the aminium ion present. The dication formed by this oxidation is the same as in the half-generation mechanism and its subsequent transformations would obviously be the same.

Kinetics provides one means to begin distinguishing amongst these four mechanisms. For example, if k_2 is rate-limiting for each of the four mechanisms, the observed kinetics would be first-order in aminium ion for the π -complex mechanism and second-order for the others. Each mechanism has two limiting kinetic extremes ($k_{-1} \ll k_2$ and $k_{-1} \gg k_2$) for a total of eight possibilities that need to be distinguished. For simplicity, we will hereafter refer to each of the four general mechanisms as I-IV and specify the kinetic possibilities within each mechanism with A and B (A for $k_{-1} \ll k_2$ and B for $k_{-1} \gg k_2$).

The kinetics of the reaction of p -An₂NCH₃^{•+}AsF₆⁻ with quinuclidine in acetonitrile were conveniently followed by monitoring the absorbance of the aminium ion at 734 nm. Although the reaction rates were too fast to be measured by conventional spectrophotometric methods, they could easily be determined by the stopped-flow technique. The kinetics were run under pseudo-first-order conditions where the quinuclidine concentration was at least in a 10-fold excess over the aminium ion salt. The solutions were maintained at a constant ionic strength by using *n*-Bu₄N⁺AsF₆⁻, although control experiments showed that the reaction rates in the presence and absence of salt were identical within experimental error.

Table III. Kinetic Data for the Reaction of p -An₂NCH₃^{•+}AsF₆⁻ with Quinuclidine in Acetonitrile at 15.1 °C

entry	p -An ₂ NCH ₃ ^{•+} AsF ₆ ⁻ × 10 ⁶ , M	quinuclidine × 10 ⁴ , M	$k_{\text{obsd}} \times 10^{-5}$, ^a M ⁻¹ s ⁻¹
1	5.0	1.49	1.2 (1)
2	5.0	2.48	1.20 (4)
3	5.0	4.96	1.06 (8)
4	3.05	6.26	1.10 (6)
5	6.1	6.26	1.04 (3)
6	15.0	6.26	0.98 (7)

^a Average of 2-4 measurements. All solutions were 3.5×10^{-3} M in *n*-Bu₄N⁺AsF₆⁻.

Table IV. Comparison of $\Delta G_{\text{et}}^\circ$ and ΔG^\ddagger for p -An₂NCH₃^{•+}AsF₆⁻ and Four Quinuclidines

base	E_p^a , V (SCE)	$\Delta G_{\text{et}}^\circ$, kcal/mol	ΔG^\ddagger , ^b kcal/mol
quinuclidine	1.11	>10	10
3-quinuclidinol	1.07	>10	11
3-chloroquinuclidine	1.37	>17	13
3-quinuclidinone	1.48	>19	14

^a In acetonitrile. $E^\circ(p\text{-An}_2\text{NCH}_3) = 0.65$ V (SCE). ^b Calculated from the rate constants in Table V using the Eyring equation.

First, the reaction order in quinuclidine was determined by varying the quinuclidine concentration and was found to be first-order in quinuclidine (Table III, entries 1-3). Second, the reaction order in aminium ion was determined at various aminium ion concentrations and was also found to be first-order (entries 4-6). These latter data exclude three mechanistic possibilities: I.B, II.B, and III.B. Five possibilities remained. These were further reduced by examining the isotope effect for the reaction of p -An₂NCH₃^{•+} vs p -An₂NCD₃^{•+}. At 15.1 °C, the kinetic isotope effect for disappearance of aminium ion was 7.68 (7).¹⁵ This is clearly a primary effect and requires cleavage of the C-H(D) bond in the rate-determining step. As such, it excludes mechanisms II.A, III.A, IV.A, and IV.B. This leaves only I.A.

In addition to mechanism I.A., the molecularity and the isotope effect studies are also consistent with one other mechanism: the variant of the electron-transfer mechanism in which the quinuclidine cation radical reacts with p -An₂NCH₃ instead of with p -An₂NCH₃^{•+}. The isotope effect requires that the hydrogen atom abstraction step be rate-limiting for this mechanism. This means that $k_{\text{obs}} = 2(k_1/k_{-1})k_2$.¹⁶ Since k_1/k_{-1} is equal to the equilibrium constant for electron transfer between p -An₂NCH₃^{•+} and quinuclidine, we thought that this mechanism might be tested by comparing the energetics of electron transfer ($\Delta G_{\text{et}}^\circ$) with the activation energy (ΔG^\ddagger) for reaction of the aminium ion salt with several quinuclidine bases. The electron-transfer mechanism requires $\Delta G_{\text{et}}^\circ < \Delta G^\ddagger$.

A comparison of $\Delta G_{\text{et}}^\circ$ and ΔG^\ddagger for p -An₂NCH₃^{•+} and four quinuclidines is given in Table IV. The data for 3-chloroquinuclidine and 3-quinuclidinone both place $\Delta G_{\text{et}}^\circ > \Delta G^\ddagger$ and thus clearly exclude the electron-transfer mechanism.¹⁷

The values of $\Delta G_{\text{et}}^\circ$ in Table IV were calculated from the oxidation potentials of p -An₂NCH₃ and of the quinuclidines obtained by cyclic voltammetry (CV). Although p -An₂NCH₃ exhibits reversible CV behavior in acetonitrile, the quinuclidines do not. The true E° values of the quinuclidines are likely to be considerably more anodic than the observed E_p 's.¹⁸ Therefore, the calculated $\Delta G_{\text{et}}^\circ$ values represent *minimum* estimates. Corrections to more realistic values would make the differences between $\Delta G_{\text{et}}^\circ$ and ΔG^\ddagger for 3-chloroquinuclidine and 3-quinuclidinone even larger than those estimated in Table IV.

(15) The standard deviation in the last digit is given in parentheses.

(16) The factor of 2 takes into account the fact that the reaction consumes two molecules of the amine cation radical.

(17) These data also exclude an electron-transfer mechanism in which hydrogen atom abstraction from p -An₂NCH₃ by the quinuclidine cation radical occurs within a solvent "cage".

(18) Nicholson, R. S.; Shain, I. *Anal. Chem.* **1964**, *36*, 706.

(14) For recent reviews, see: (a) Bard, A. J.; Ledwith, A.; Shine, H. J. *Adv. Phys. Org. Chem.* **1976**, *13*, 156. (b) Hammerich, O.; Parker, V. D. *Adv. Phys. Org. Chem.* **1984**, *20*, 55. (c) Parker, V. D. *Acc. Chem. Res.* **1984**, *17*, 243.

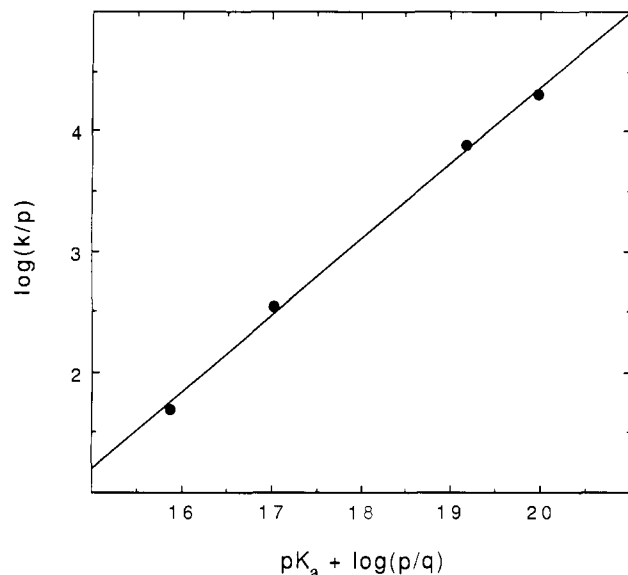


Figure 4. Brønsted plot for deprotonation of $p\text{-An}_2\text{NCH}_3^+\text{AsF}_6^-$ by quinuclidine in acetonitrile at 15.1 °C.

Table V. Kinetic Isotope Effects at 15.1 °C

base	pK_a^a	$k_H^b \times 10^{-2}$, $M^{-1} s^{-1}$	k_H/k_D^b
quinuclidine	19.51	615 (1)	7.68 (7)
3-quinuclidinol	18.70	227 (3)	8.56 (8)
3-chloroquinuclidine	16.55	10.4 (1)	9.0 (3)
3-quinuclidinone	15.40	1.50 (3)	6.0 (5)

^aIn acetonitrile.¹⁹ ^b $k_H = k_{\text{obs}}/2$. Rate constants at 15.1 °C.

Although the data for quinuclidine and 3-quinuclidinol do not permit a similarly definitive mechanistic conclusion, any appreciable activation energy for electron transfer would predict a rate below that experimentally observed. More compelling evidence for a common reaction mechanism for all four quinuclidines comes from a Brønsted plot (Figure 4), which shows excellent linearity. This plot also provides additional qualitative support for a rate-limiting proton-transfer mechanism. The β value obtained from the slope of this plot (0.63) suggests that the transition state for proton transfer is reasonably well-advanced.

As a further probe of the transition-state structures, we determined the relative kinetic isotope effects for the four quinuclidines. Interestingly, the isotope effects do not follow the trend in pK_a of the quinuclidines¹⁹ (Table V). Figure 5 shows a plot of the data with the best least-squares fit to a quadratic equation.²⁰ One possible explanation for the bell-shaped isotope effect curve is that the amine cation radical has a pK_a near the isotope effect maximum ($pK_a \approx 17.7$), where the transition state is expected to be most symmetrical. This explanation seemed unlikely to us since no break was observed in the Brønsted plot near $pK_a \approx 18$. To test this hypothesis further, we decided to determine the pK_a of the amine cation radical. This was done by using eq 1⁹ where

$$(pK_a)_{\text{CH}_3\text{CN}} = \frac{-E_{\text{CH}_3\text{CN}}^\circ}{0.05916} + \frac{\Delta G_{\text{BDE}}^\circ - 37.5}{1.36} \quad (1)$$

$E_{\text{CH}_3\text{CN}}^\circ$ is the oxidation potential of the amine vs NHE and $\Delta G_{\text{BDE}}^\circ$ is the standard free energy for the gas-phase bond dissociation energy of the C–H bond α to nitrogen. The oxidation potential of the amine in acetonitrile was obtained by cyclic voltammetry (0.65 V vs SCE; 0.89 V vs NHE). The bond dissociation free energy was determined by first estimating $\Delta H_{\text{BDE}}^\circ$. This was done by using photoacoustic calorimetry to measure the heats of reaction for hydrogen abstraction from Ph_2NCH_3 and

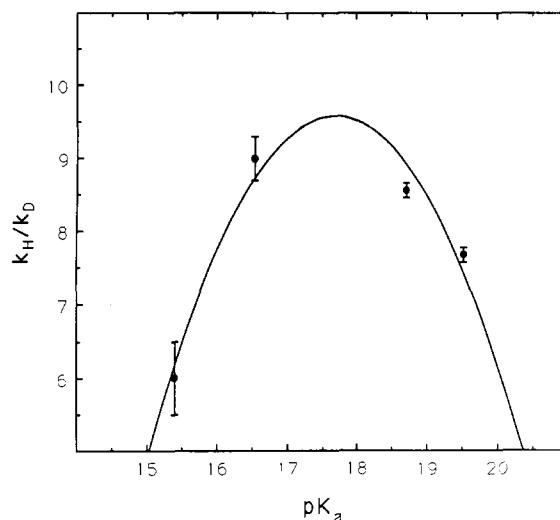


Figure 5. Isotope effects for deprotonation of $p\text{-An}_2\text{NCH}_3(\text{CD}_3)^+\text{AsF}_6^-$ by substituted quinuclidines.

from Et_3N by benzophenone triplet.²¹ In practice, we found that these two abstractions deposited the same amount of energy within experimental error (± 2 kcal/mol). The C–H bond strength of Et_3N was estimated from the work of Lossing to be 80 kcal/mol.²² This estimate and the photoacoustic data place $\Delta H_{\text{BDE}}^\circ$ for Ph_2NCH_3 at 80 kcal/mol. We approximated the bond dissociation entropy ($\Delta S_{\text{BDE}}^\circ$) by assuming that it is equal to the standard entropy of the hydrogen atom (27.4 cal/mol-deg).⁹ Combining the estimates of $\Delta H_{\text{BDE}}^\circ$ and $\Delta S_{\text{BDE}}^\circ$ gives $\Delta G_{\text{BDE}}^\circ \approx 72$ kcal/mol at 25 °C. This, in turn, provides a pK_a for $p\text{-An}_2\text{NCH}_3^+$ of 10 in acetonitrile. Although this pK_a estimate is somewhat approximate, it seems clear that the isotope effect maximum in Figure 5 does not occur at $\Delta pK_a = 0$.

The pK_a estimate for $p\text{-An}_2\text{NCH}_3^+$ requires that the isotope effect maximum be reached when the proton transfer is exothermic by ca. 8 pK_a units. This is rather unusual since isotope effect maximums for proton transfers are typically observed at $\Delta pK_a \approx 0$.²³ One difference between $p\text{-An}_2\text{NCH}_3^+$ and more typical carbon acids is that the C–H bond being cleaved during proton transfer is significantly weaker for $p\text{-An}_2\text{NCH}_3^+$ than for most carbon acids.

The homolytic bond dissociation energy of the N -methyl C–H bond in $p\text{-An}_2\text{NCH}_3^+$ can be calculated from the thermodynamic cycle below.⁷ Three quantities are needed to calculate the bond dissociation energy of the cation radical: (1) the oxidation potential of the amine ($E^\circ = 0.65$ V vs SCE), (2) the homolytic bond dissociation energy of the neutral amine ($\Delta H_{\text{BDE}}^\circ = 80$ kcal/mol), and (3) the oxidation potential of the α -amino radical ($E_p = -0.79$ V vs SCE). The latter value was obtained by determining the reduction potential of $p\text{-An}_2\text{N}=\text{CH}_2^+\text{BF}_4^-$ in acetonitrile. These numbers provided an estimate of 47 kcal/mol for the bond dissociation energy of the N -methyl C–H bond in $p\text{-An}_2\text{NCH}_3^+$.

(21) The photoacoustic measurements were made in acetone by using the apparatus described previously: Herman, M. S.; Goodman, J. L. *J. Am. Chem. Soc.* **1989**, *111*, 1849. The quantum yields needed for the photoacoustic work were determined for both abstraction reactions by monitoring the amount of benzhydryl radical formed at 540 nm by nanosecond flash photolysis. The hydrogen atom abstraction from benzhydryl by triplet benzophenone ($\Phi = 2.0$) was used as a reference actinometer: Inbar, S.; Linshitz, H.; Cohen, S. G. *J. Am. Chem. Soc.* **1981**, *103*, 1048. The abstraction reactions from Et_3N and Ph_2NCH_3 were both found to have a quantum yield of 1.0 within experimental error. We should point out that we could not determine the BDE of $p\text{-An}_2\text{NCH}_3$ in a similar way because the absorbance of the amine interfered with the absorbance of benzophenone.

(22) Burkey, T. J.; Castelano, A. L.; Griller, D.; Lossing, F. P. *J. Am. Chem. Soc.* **1983**, *105*, 4701. The α -C–H bond dissociation energy of Et_3N was estimated by taking the BDE of Me_3N (84 kcal/mol) and subtracting the incremental effect of α -methyl substitution (4 kcal/mol).

(23) (a) Bell, R. P. *The Proton in Chemistry*, 2nd ed.; Cornell University Press: Ithaca, NY, 1973; Chapter 12. (b) Melander, L.; Saunders, W. H., Jr. *Reaction Rates of Isotopic Molecules*; Wiley: New York, 1980; Chapter 5. (c) Reference 20.

(19) Beltrame, P.; Gelli, G.; Loi, A. *Gazz. Chim. Ital.* **1980**, *110*, 491.

(20) For the theoretical significance of a quadratic relationship between k_H/k_D and pK_a , see: More O'Ferrall, R. A. In *Proton-Transfer Reactions*; Caldin, E. F.; Gold, V., Eds.; Chapman and Hall: London, 1975; Chapter 8.

Table VI. Activation Parameters for the Reaction of $p\text{-An}_2\text{NCH}_3^{+\bullet}\text{AsF}_6^-$ and $p\text{-An}_2\text{NCD}_3^{+\bullet}\text{AsF}_6^-$ with Quinuclidine and 3-Quinuclidinone in Acetonitrile

Param	quinuclidine ^a		3-quinuclidinone ^a	
	Protio	Deuterio	Protio	Deuterio
ΔH^\ddagger , kcal mol ⁻¹	3.7 (1)	5.21 (9)	5.70 (4)	7.10 (3)
ΔS^\ddagger , cal/mol-deg	-22.3 (4)	-21.2 (3)	-30.7 (2)	-29.9 (1)
A , M ⁻¹ s ⁻¹	$2.1 (4) \times 10^8$	$3.7 (5) \times 10^8$	$3.0 (2) \times 10^6$	$4.7 (2) \times 10^6$
E_a , kcal mol ⁻¹	4.3 (1)	5.78 (8)	6.24 (4)	7.68 (3)
A_H/A_D	0.57 (13)		0.64 (5)	

^a Activation parameters were obtained from a nonlinear least-squares fit of $k_{\text{obs}}/6$ to the Eyring or Arrhenius equation. Rates were measured at five temperatures between -35 and +30 °C.

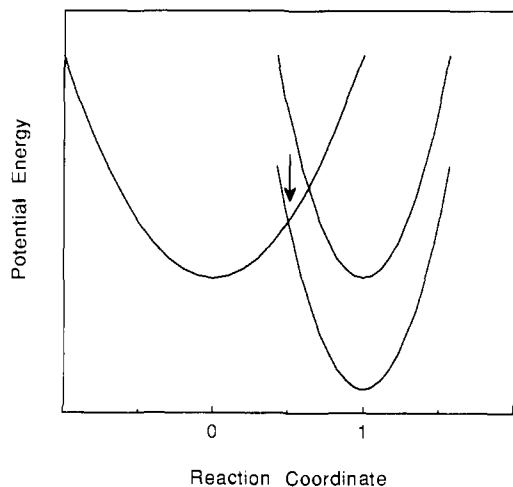
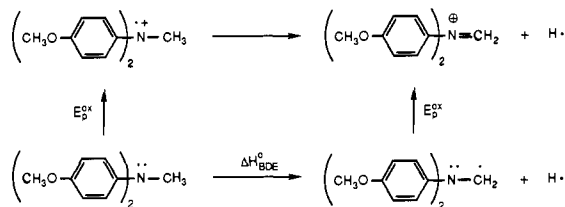


Figure 6. Reaction coordinate diagram. The reaction coordinate at 0.5 is marked by the arrow.

This should probably be considered an *upper* limit since the true reduction potential of the iminium ion is likely more cathodic than the observed E_p .



In contrast to the weak C-H bond broken during proton transfer, the N-H bond made to quinuclidine is quite strong, 97 kcal/mol.²⁴ The much smaller bond energy of the bond being broken suggests that the potential energy well for the reactant is considerably wider than for the product. The consequence of this is graphically shown in Figure 6. It is clear from this diagram that a symmetrical transition state will be attained only when the proton transfer is exothermic. This explanation nicely rationalizes our isotope effect data. It also suggests that this behavior may be common for proton transfers from cation radicals.

For example, this explanation may also rationalize the isotope effect maximum reported for the deprotonation of the 1-benzyl-1,4-dihydro-2-pyridinamide cation radical by substituted pyridine bases.²⁵ In this case, an isotope effect maximum was observed at $\text{p}K_a \approx 10.4$ in acetonitrile.²⁶ The authors explained this observation by assuming that the cation radical had a $\text{p}K_a$ close to where the $\text{p}K_a$ maximum was observed. This explanation appears incorrect. We have estimated the $\text{p}K_a$ of the cation radical

(24) Staley, R. H.; Beauchamp, J. L. *J. Am. Chem. Soc.* **1974**, *96*, 1604.

(25) Fukuzumi, S.; Kondo, Y.; Tanaka, T. *J. Chem. Soc., Perkin Trans. 2* **1984**, 673.

(26) The pyridine acidities quoted in ref 25 refer to $\text{p}K_a$'s in water. The isotope effects, however, were determined in acetonitrile. A linear regression analysis of pyridine $\text{p}K_a$'s in acetonitrile (Cauquis, G.; Deronzier, A.; Serve, D.; Vieil, E. *J. Electroanal. Chem. Interfacial Electrochem.* **1975**, *60*, 205) with those in water gave: $\text{p}K_a(\text{CH}_3\text{CN}) = 1.31\text{p}K_a(\text{H}_2\text{O}) + 5.41$ (corr coeff = 0.9993). We used this empirical correlation to estimate the isotope effect maximum in acetonitrile.

by using eq 1 and found that it has a $\text{p}K_a$ considerably less than 10. By using the oxidation potential of 1-benzyl-1,4-dihydro-2-pyridinamide in acetonitrile ($E^\circ = 0.89$ vs SCE; 1.03 vs NHE),²⁷ and an estimate for $\Delta H_{\text{BDE}}^\circ(\text{C}_4\text{-H})$ of 74 kcal/mol,²⁸ we calculated a $\text{p}K_a$ of 3.5 for the cation radical. Thus the isotope effect maximum appears to occur when the proton transfer is exothermic by ca. 7 $\text{p}K_a$ units. This result is readily explained by Figure 6.

The magnitude of the isotope effects we obtained for the reaction of $p\text{-An}_2\text{NCH}_3(\text{CD}_3)^{+\bullet}$ with the four quinuclidines ($k_H/k_D = 6.0\text{--}9.0$) seemed large to us when compared to the isotope effects reported for the deprotonation of other amine cation radicals ($k_H/k_D \approx 2\text{--}5$).²⁹ Tunneling seemed like one possible explanation for the larger isotope effects observed in our case. To test this possibility, we examined the temperature dependences of the isotope effects for quinuclidine and 3-quinuclidinone. Table VI contains the Arrhenius preexponential factors needed to assess the tunneling contribution. Neither of the A_H/A_D ratios—0.57 for quinuclidine and 0.64 for 3-quinuclidinone—provided compelling evidence for tunneling, although they are in the upper part of the range normally associated with a tunneling contribution.^{23b}

In addition to A_H and A_D , Table VI contains the remainder of the activation parameters for reaction of $p\text{-An}_2\text{NCH}_3(\text{CD}_3)^{+\bullet}\text{AsF}_6^-$ with quinuclidine and 3-quinuclidinone. These data show that the activation free energies for both quinuclidines are dominated by the entropy terms over the temperature range studied here. Although large, the negative activation entropies are comparable to those observed for other deprotonations at carbon by amine bases in acetonitrile.³⁰ Finally, we should point out that these data represent, to the best of our knowledge, the first determination of the activation parameters for the deprotonation of an organic cation radical. They also nicely illustrate one of the advantages of preparing isolable salts for the detailed investigation of cation-radical reactions.

Returning to the isotope effects, it is not yet clear what significance may be ascribed to the differences in isotope effects that have been reported for the deprotonation of amine cation radicals. The cation radicals and bases studied to date span a range of structure and few studies employing systematic structural variations have been made. Nonetheless, the magnitudes of the isotope effects we have obtained for the deprotonation of $p\text{-An}_2\text{NCH}_3^{+\bullet}$

(27) This oxidation potential has been recommended by: Miller, L. L.; Valentine, J. R. *J. Am. Chem. Soc.* **1988**, *110*, 3982.

(28) The $\text{C}_4\text{-H}$ BDE was estimated by AM1 calculation: Dewar, M. J. S.; Zoebisch, E. G.; Healy, E. F.; Stewart, J. J. P. *J. Am. Chem. Soc.* **1985**, *107*, 3902. By using the AM1-estimated heat of formation of the hydrogen atom (57.1 kcal/mol), 1-benzyl-1,4-dihydro-2-pyridinamide (-7.3 kcal/mol), and its radical (9.7 kcal/mol), the BDE was calculated to be 74 kcal/mol. $\Delta G_{\text{BDE}}^\circ$ was estimated by using the approximation for $\Delta S_{\text{BDE}}^\circ$ in the text. For comparison, a similar calculation for trimethylamine gave a BDE for the C-H bond of 83 kcal/mol. This compares well with two experimental estimates: 84 kcal/mol²² and 85 kcal/mol (Grela, M. A.; Colussi, A. J. *Int. J. Chem. Kinet.* **1985**, *17*, 257).

(29) (a) Hull, L. A.; Davis, G. T.; Rosenblatt, D. H.; Williams, H. K. R.; Weglein, R. C. *J. Am. Chem. Soc.* **1967**, *89*, 1163. (b) Lindsay Smith, J. R.; Mead, L. A. V. *J. Chem. Soc., Perkin Trans. 2* **1973**, 206. (c) Lindsay Smith, J. R.; Masheder, J. J. *J. Chem. Soc., Perkin Trans. 2* **1976**, 47. (d) Lewis, F. D.; Ho, T.-I. *J. Am. Chem. Soc.* **1980**, *102*, 1751. (e) Reference 4d. (f) Powell, M. F.; Wu, J. C.; Bruce, T. C. *J. Am. Chem. Soc.* **1984**, *106*, 3850. (g) Reference 10.

(30) (a) Caldin, E. F.; Mateo, S. *J. Chem. Soc., Chem. Commun.* **1973**, 854. (b) Caldin, E. F.; Mateo, S. *J. Chem. Soc., Faraday Trans. 1* **1975**, *71*, 1876. (c) Jarczewski, A.; Pruszyński, P.; Kazi, M.; Leffek, K. T. *Can. J. Chem.* **1984**, *62*, 954.

may have an impact on the interpretation of several cytochrome P-450 and peroxidase-catalyzed oxidations of tertiary amines. For example, the enzyme-catalyzed oxidations of *N*-methyl-*N*-(trideuteriomethyl)aniline have been suggested to proceed via an amine cation-radical deprotonation mechanism if the observed intramolecular isotope effect was between 2 and 3 and to proceed via hydrogen atom abstraction from the neutral amine if the isotope effect was larger (e.g., 8–10). The isotope effects we have directly measured for the deprotonation of *p*-An₂NCH₃^{•+} by the quinuclidine bases lie in or near this latter range (Table V) and suggest that this mechanistic criterion should be viewed with caution. Clearly, the structure of the cation radical, the base, and the nature of the surrounding medium need to be taken into consideration when interpreting the isotope effects for these reactions.

In order to make more detailed comparisons of our work on the deprotonation of *p*-An₂NCH₃^{•+} with other tertiary amine cations, it would be necessary to have activation parameters, isotope effects, Brønsted coefficients, etc., for other amine cation radical deprotonations. Unfortunately, such detailed data are not presently available. In the absence of this data, perhaps the best way to compare the various amine cation radicals is by their *pK*_a's. In principle, these *pK*_a's can be estimated by using eq 1. One problem with this approach is that these estimates are necessarily approximate since the oxidations of most tertiary amines are not reversible.³¹ Here we will make what is admittedly a crude comparison of the *pK*_a of *p*-An₂NCH₃^{•+} to that of a tertiary amine cation radical commonly accepted to be highly reactive, PhN(CH₃)₂^{•+}. When an oxidation potential of 0.95 V (*E*_{p/2} vs NHE) is used for PhN(CH₃)₂^{•+} and it is assumed that the C–H bond dissociation energy is the same as for the Ph₂NCH₃ (80 kcal/mol), eq 1 provides a *pK*_a for PhN(CH₃)₂^{•+} of 9. Although this estimate must be considered very approximate, it is similar to that estimated for *p*-An₂NCH₃^{•+} (*pK*_a = 10) and suggests that the results we have obtained with *p*-An₂NCH₃^{•+}AsF₆⁻ may be relevant to other reactive amine cation radicals.

Finally, we should make some mention of the rate constants that we have measured for the deprotonation of *p*-An₂NCH₃^{•+}. The rate constants for deprotonation by all four quinuclidines are well below the diffusion-controlled limit (ca. 10¹⁰ in acetonitrile at 25 °C) despite the fact that all of these proton transfers are calculated to be exothermic. This suggests that, despite the acidifying effect of one-electron oxidation, *p*-An₂NCH₃^{•+} is a rather typical carbon acid; i.e., its rate of proton transfer is unusually slow relative to a "normal"³² acid. This property also appears to be shared by alkylaromatic cation radicals.^{1a} On the other hand, the large entropic contributions to the activation energy that we have measured for *p*-An₂NCH₃^{•+} suggest that proton transfer would be much more rapid under conditions in which the contributions to Δ*S*[‡] were minimized. It seems reasonable that this condition might be met for proton transfer within ion radical pairs/excplexes, and this may explain the rapid proton-transfer rates reported for amine cation radicals within these complexes.³³

Conclusions

In summary, the preparation of *p*-An₂NCH₃^{•+}AsF₆⁻ has permitted the direct examination of the reaction of a tertiary amine cation radical with bases. This has allowed the determination of rate constants, activation parameters, Brønsted parameters, and isotope effects for the deprotonation reaction. It should be possible to apply this approach to other cation radical deprotonations that are difficult to probe by more traditional kinetic methods.

Experimental Section

General Methods. ¹H NMR spectra were recorded with either a General Electric/Nicolet QE-300 spectrometer or a Bruker WH-400 spectrometer. Proton chemical shifts are reported in ppm downfield from tetramethylsilane. Proton-proton coupling constants reflect assumed first-order behavior. EPR spectra were acquired with 100-kHz modu-

lation using a Bruker ESR-200D spectrometer, equipped with a Hewlett-Packard 5342a microwave frequency counter and interfaced to an IBM PC-AT. Inert-atmosphere manipulations were conducted under nitrogen in a Vacuum Atmospheres HE-43-2 DRI-LAB glovebox equipped with a Vacuum Atmospheres HE-493 DRI-TRAIN. Stopped-flow kinetic measurements were performed on a Hi-Tech Scientific instrument composed of a SF-3L support unit, SF-40C spectrophotometer control unit, and a TDU-43 timer delay unit. The instrument was interfaced to an Apple II Plus computer. The Apple II Plus was connected to a Digital Equipment Corp. VAX-750 minicomputer via an Apple Super Serial Card interface. Kinetic data were transferred to the VAX-750 where they were fit with a nonlinear least-squares program. Bath temperatures were measured with a Fisher Model R-250C RTD digital thermometer using a platinum RTD probe. Cyclic voltammograms were obtained using a Bioanalytical Systems Model DCV-4 voltammetry instrument and recorded on a Hewlett-Packard 7015B X-Y recorder. Cyclic voltammetry measurements were performed in a homemade electrochemical cell employing a platinum disk (1.5-mm diameter) working electrode, a platinum gauze (7.5 mm × 10 mm) auxiliary electrode, and a coiled silver wire as the reference electrode. All potentials were referenced to internal ferrocene (0.307 V vs SCE).³⁴ All measurements were made in acetonitrile with tetra-*n*-butylammonium hexafluorophosphate (0.1 M) as the supporting electrolyte using a scan rate of 150 mV/s.

Materials. Diethyl ether was distilled from sodium benzophenone ketyl under nitrogen. Chlorodifluoromethane (Matheson) was stirred over phosphorus pentoxide at -78 °C and vacuum transferred before use. Acetonitrile was distilled under nitrogen successively from aluminum trichloride, potassium permanganate/lithium carbonate, potassium bisulfite, calcium hydride, and phosphorus pentoxide and then stored under nitrogen.³⁵ Methylene chloride was refluxed under nitrogen with aluminum trichloride for 2 h, cooled, and allowed to settle overnight. After decanting, the methylene chloride was washed with water, dried over calcium chloride, distilled from phosphorus pentoxide, and stored under nitrogen.³⁶ Tetra-*n*-butylammonium hexafluoroarsenate (Ozark-Mahoning) was recrystallized from methylene chloride/hexanes (2:3) and dried [80 °C (0.03 mmHg)]. Dioxygenyl hexafluoroarsenate (Ozark-Mahoning) was used as received. Quinuclidine (Aldrich) was sealed in vacuo with an equivalent weight of freshly cut sodium metal, heated to 180 °C (4 h), and then sublimed. 3-Quinuclidinol (Aldrich) was sublimed [90 °C (0.03 mmHg)] prior to use. 3-Chloroquinuclidine hydrochloride and 3-quinuclidinone hydrochloride (Aldrich) were stirred as slurries in diethyl ether over potassium hydroxide to obtain the free bases. The ether solutions were then washed with brine and dried over anhydrous magnesium sulfate. After filtration, the ether was evaporated. 3-Chloroquinuclidine was distilled [100 °C (0.03 mmHg)] to give a white solid. 3-Quinuclidinone was sublimed [90 °C (0.03 mmHg)] to give a white solid.

Preparation of Di-*p*-anisylmethylamine (*p*-An₂NCH₃). A 25-mL round-bottomed flask equipped with a condenser was charged with 0.538 g (2.35 mmol) of di-*p*-anisyl amine,³⁷ 0.0874 g (0.237 mmol) of tetra-*n*-butylammonium iodide, 0.300 g (5.35 mmol) of potassium hydroxide, 5.0 mL of benzene, and 0.05 mL of water. Under nitrogen, the flask was heated to 88 °C for 1 h to dissolve the ammonium salt and then cooled to room temperature. Iodomethane (0.160 mL) was added dropwise (2 min), and the reddish brown solution was reheated to reflux (2 h). Then additional tetra-*n*-butylammonium iodide (85.0 mg, 0.230 mmol) and potassium hydroxide (0.1057 g, 1.88 mmol) were charged to the flask, which was reheated to reflux (3 h). After cooling, the benzene solution was decanted and washed successively with 20-mL portions of water, 5% aqueous sodium carbonate, and brine and was dried over anhydrous sodium sulfate. Filtration and solvent removal in vacuo gave a tan solid (0.546 g). Chromatography on silica gel using 80:20 hexane/diethyl ether as an elutant gave, after solvent removal, white needles (0.40 g, 70%). MP: 99–99.5 °C (lit.³⁸ mp 99 °C). ¹H NMR (CDCl₃): δ 6.92 (d, *J* = 9.0 Hz, 3.92 H), 6.84 (d, *J* = 9.0 Hz, 3.92 H), 3.79 (s, 6.13 H), 3.24 (s, 3.02 H).

Di-*p*-anisylmethylamine-*d*₃ was similarly prepared using iodomethane-*d*₃ (99.5+ atom % D, Aldrich).

Preparation of Di-*p*-anisylmethylaminium Hexafluoroarsenate (*p*-An₂NCH₃^{•+}AsF₆⁻). In the glovebox, a U-tube, which was divided by a break-seal, was charged on one side with 45.9 mg (0.189 mmol) of

(34) Bard, A. J.; Faulkner, L. R. *Electrochemical Methods*; Wiley: New York, 1980.

(35) Walter, M.; Ramaley, L. *Anal. Chem.* **1973**, *45*, 165.

(36) Jones, D. E. H.; Wood, J. L. *J. Chem. Soc. A* **1966**, 1448.

(37) Chen, M. M.; D'Adamo, A. F.; Walter, R. I. *J. Org. Chem.* **1961**, *26*, 2721.

(38) Imperial Chemical Industries Ltd. German Patent 665,921, **1938**; *Chem. Abstr.* **1939**, *33*, 1543.

(31) Nelsen, S. F.; Hintz, P. J. *J. Am. Chem. Soc.* **1972**, *94*, 7114.

(32) Eigen, M. *Angew. Chem., Int. Ed. Engl.* **1964**, *3*, 1.

(33) (a) Shaefer, C. G.; Peters, K. S. *J. Am. Chem. Soc.* **1980**, *102*, 7566.

(b) Hub, W.; Schneider, S.; Dörr, F.; Oxman, J. D.; Lewis, F. D. *J. Am. Chem. Soc.* **1984**, *106*, 708.

di-*p*-anisylmethylamine and on the other side with 43.0 mg (0.195 mmol) of dioxygenyl hexafluoroarsenate. The tube was capped, removed from the glovebox, and attached to a high-vacuum line where it was evacuated. Chlorodifluoromethane (1.7 mL) was vacuum transferred into the side containing the amine. With the tube at -130°C , the break-seal was broken. A green color developed instantly and darkened upon stirring. After 25 min, the solvent was removed in vacuo, and the apparatus was allowed to warm to room temperature. The green solid that remained was dissolved in 20 mL of a 1:6 acetonitrile/methylene chloride solution and, under nitrogen, the solution was equally divided into six septum-capped test tubes. Diethyl ether (6.2 mL) was mixed into each tube, and an additional 5.4 mL of ether was layered on top of the mixed solutions. The test tubes were placed in a -20°C freezer. After 14 h, purple, metallic-looking needles formed. The mother liquor was removed using a Teflon-needled syringe, and the crystals were rinsed with two 2-mL portions of diethyl ether. The solvent was removed in vacuo. Yield: 57.5 mg (70.4%). MP: $90-95^{\circ}\text{C}$ dec. Anal. Calcd for $\text{C}_{15}\text{H}_{17}\text{NO}_2\text{AsF}_6$: C, 41.68; H, 3.96; N, 3.24. Found: C, 41.51; H, 3.93; N, 3.17. A degassed EPR sample was prepared in methylene chloride (10^{-4} M). EPR (CH_2Cl_2): $a_{\text{N}} = 9.97$ G, $a_{\text{CH}_3} = 10.46$ G, $a_0 = 2.49$ G, $a_m = 0.50$ G, $a_p = 1.00$ G (lit.¹¹ EPR (CH_3CN): $a_{\text{N}} = 9.77$ G, $a_{\text{CH}_3} = 10.27$ G, $a_0 = 2.42$ G, $a_m = 0.48$ G, $a_p = 0.97$ G).

Preparation of *N*-[(Di-*p*-anisylamino)methyl]quinuclidinium Tetrafluoroborate (1). A solution of 35.0 mg (0.144 mmol) of di-*p*-anisylmethylamine in 1.0 mL of acetonitrile was added dropwise to a solution of 46.3 mg (0.140 mmol) of triphenylcarbenium tetrafluoroborate in 1.0 mL of acetonitrile under a nitrogen atmosphere. After stirring for 30 min, 10.0 mL of carbon tetrachloride was added and a light green oil separated. The solvents were evaporated to give a light green solid. The solid was rinsed with six 1-mL portions of carbon tetrachloride to remove triphenylmethane (36 mg). The remaining solid was analyzed by NMR. ^1H NMR (CDCl_3): δ 8.24 (s, 1.94 H), 7.48 (d, $J = 9.0$ Hz, 4.04 H), 7.02 (d, $J = 9.0$ Hz, 3.92 H), 3.87 (s, 6.10 H). The solid was then dissolved in 2 mL of methylene chloride, and a solution of quinuclidine (17.9 mg, 0.161 mmol) in 2 mL of methylene chloride was added. After 5 min a flocculent precipitate formed. The solvent was removed by rotary evaporation to give an off-white solid. ^1H NMR (CD_3CN): δ 7.08 (d, $J = 7.0$ Hz, 4.01), 6.90 (d, $J = 7.0$ Hz, 3.97 H), 5.09 (s, 1.98 H), 3.78 (s, 5.85 H), 3.40 (m, 6.06 H), 2.17 (m, 1.04 H), 1.98 (m, 6.10 H).

Reaction of Di-*p*-anisylmethylaminium Hexafluoroarsenate with

Quinuclidine in Acetonitrile. A solution of di-*p*-anisylmethylaminium hexafluoroarsenate (3.0 mg, 0.012 mmol) in 1.5 mL of acetonitrile was added via syringe over 2 min to a solution containing 13.5 mg (0.121 mmol) of quinuclidine in 1.5 mL of acetonitrile. The aminium ion solution decolorized immediately upon addition. After 10 min, the solvent and excess quinuclidine were removed in vacuo. ^1H NMR analysis showed three products, *N*-[(di-*p*-anisylamino)methyl]quinuclidinium hexafluoroarsenate (1), di-*p*-anisylmethylamine, and quinuclidinium hexafluoroarsenate. The first two products were identified by comparison with authentic spectra. The quinuclidinium hexafluoroarsenate was identified by addition of a small quantity of quinuclidinium chloride, which increased the peak intensities at δ 3.12 (br t, $J = 8.1$ Hz), 2.00 (sept, $J = 3.23$ Hz), and 1.79 (br dt). The yields of *N*-[(di-*p*-anisylamino)methyl]quinuclidinium hexafluoroarsenate (1) (48%) and di-*p*-anisylmethylamine (49%) were determined by ^1H NMR integration against an internal standard (fluorenone).

Stopped-Flow Kinetics. The reaction kinetics were performed on freshly prepared solutions, which were stored under a nitrogen atmosphere. Both the aminium ion and the base solutions contained tetra-*n*-butylammonium hexafluoroarsenate (3.5 mM). The disappearance of aminium ion was followed at 734 nm. During temperature-dependent runs, the instrument was allowed to equilibrate for at least 1 h after reaching the desired temperature.

Acknowledgment. We thank J. L. Goodman for assistance in the photoacoustic measurements, I. R. Gould for the quantum yield determinations, W. D. Jones for help in the X-ray structure analysis, and W. H. Saunders, Jr., for the use of his stopped-flow spectrophotometer. Research support was provided by the National Science Foundation (Grant CHE86-10404) and by the National Institutes of Health (Grant S07 RR07069-23).

Supplementary Material Available: Tables of X-ray data for *p*-An₂NCH₃⁺AsF₆⁻ including listings of intramolecular bond angles and bond distances, intermolecular distances, least-squares planes, torsion and conformation angles, and positional and thermal parameters (7 pages); listing of observed and calculated structure factors (8 pages). Ordering information is given on any current masthead page.

Lewis Acid Catalysis of Photochemical Reactions. 8. Photodimerization and Cross-Cycloaddition of Coumarin¹

Frederick D. Lewis* and Steven V. Barancyk

Contribution from the Department of Chemistry, Northwestern University,
Evanston, Illinois 60208-3113. Received May 8, 1989

Abstract: The effect of Lewis acid complexation upon the electronic structure and photochemical behavior of coumarin has been investigated. Changes in IR and ^1H NMR spectra upon complexation of coumarin with BF_3 or EtAlCl_2 are indicative of 1:1 complexation of the Lewis acid with the carbonyl oxygen. Changes in the UV spectrum and the observation of room-temperature fluorescence from the coumarin- BF_3 complex are attributed to increased energy of the n,π^* singlet state relative to the fluorescent π,π^* singlet state. Dimerization is found to occur via the reaction of either the singlet or triplet complex with ground-state coumarin. The singlet-state reaction selectively yields the syn head-to-tail dimer while the triplet-state reaction yields the anti head-to-head dimer. The singlet- and triplet-state complexes also react with simple alkenes. Addition of the singlet complex with the isomeric 2-butenes occurs with retention of configuration. The enhanced reactivity of complexed vs uncomplexed coumarin is attributed to its increased singlet-state lifetime and electrophilicity.

The photophysical and photochemical behavior of coumarin and its derivatives have been the subject of numerous investigations. Direct irradiation of the parent unsubstituted coumarin in solution results in highly inefficient photodimerization and cross-cycloaddition with simple alkenes, whereas triplet sensitization results in more efficient reactions.²⁻⁹ These observations

are consistent with the absence of fluorescence and low efficiency of intersystem crossing from the short-lived singlet state in non-

(1) Part 7: Lewis, F. D.; Quillen, S. L.; Hale, P. D.; Oxman, J. D. *J. Am. Chem. Soc.* **1988**, *110*, 1261.

(2) (a) Schenck, G. O.; von Wilucki, I.; Krauch, C. H. *Chem. Ber.* **1962**, *95*, 1409. (b) Krauch, C. H.; Farid, S.; Schenck, G. O. *Chem. Ber.* **1966**, *99*, 625.

(3) Hammond, G. S.; Stout, C. A.; Lamola, A. A. *J. Am. Chem. Soc.* **1964**, *86*, 3103.

(4) (a) Morrison, H.; Curtis, H.; McDowell, T. *J. Am. Chem. Soc.* **1966**, *88*, 5415. (b) Hoffman, R.; Wells, P.; Morrison, H. *J. Org. Chem.* **1971**, *36*, 102. (c) Morrison, H.; Hoffman, R. *J. Chem. Soc., Chem. Commun.* **1968**, 1453.

(5) Muthuramu, K.; Ramamurthy, V. *J. Org. Chem.* **1982**, *47*, 3976.

(6) Schenck, G. O.; Hartmann, W.; Mannsfeld, S.-P.; Metzner, W.; Krauch, C. H. *Chem. Ber.* **1962**, *95*, 1642.